American Mineralogist, Volume 70, pages 814–821, 1985

Order–disorder structure and the internal texture of stilbite

MIZUHIKO AKIZUKI AND HIROSHI KONNO

Institute of Mineralogy, Petrology, and Economic Geology
Faculty of Science, Tohoku University, Sendai 980, Japan

Abstract

Stilbite crystals from three localities (Eyi Ju, North Korea, Bomeki, Japan and Poona, India) consist of various growth sectors. With regard to X-rays, the {001} sector is orthorhombic, whereas the {110} sector is monoclinic, though the crystals are chemically homogeneous. Optical study shows that stilbite is triclinic throughout the crystal. The relationship between the orthorhombic and monoclinic symmetries may be explained by order-disorder of tetrahedron rotations which occur during growth. Small deviations from monoclinic symmetry may be due to Al/Si ordering. The sector twinning is explained by growth ordering.

Introduction

Stilbite is a common zeolite; the chemical formula is $(Na,K)_x(Ca,Mg)_{4+y}Al_{x+8+2y}Si_{28-x-2y}O_{72} \cdot 28H_2O$ with $\alpha < 4.89$ and $-2.22 < y < +0.33$ (Passaglia et al., 1978). There is no compositional gap between stilbite (a monoclinic sodium-rich phase) and stellerite (an orthorhombic sodium-poor phase).

In some minerals, the symmetry as determined by optics is lower than that determined by X-ray diffraction. Such an optical property has been called an optical anomaly. Langeman (1886) studied the optics of stilbite, and found that it is triclinic. However, stilbite has been considered to be monoclinic in X-ray work; Breck (1974) reported the space group $C2/m$, and Slaughter (1970) and Galli (1971) reported the space groups $C2$ or Cm. Langeman (1886) observed sectors corresponding to the crystal macro-faces and recognized the triclinic nature of stilbite, but did not observe the surface growth patterns and corresponding domains within the sectors. Based on studies of the relation between surface feature and internal texture, Akizuki and Sunagawa (1978), Akizuki et al. (1979), Akizuki (1981a, b) and Akizuki (1984) have explained the optical properties and internal textures of some minerals by atomic ordering produced on side faces of growth steps, suggesting a general mechanism for sector growth.

Optical observation

Both the Bomeki and Eyi Ju specimens were obtained from the same hand specimens that were analyzed by wet chemical methods. The Poona stilbites were analyzed by one of the present writers (Konno) (Table 1). Some optical observations of Bomeki stilbite were carried out by Akizuki (1980). Different authors have used different crystal settings for stilbite, and even in the usual settings for monoclinic stilbite and orthorhombic stellerite, the crystal axes are not comparable (Kerr, 1977). Figure 1 shows the orientation used in the present study. In some figures, the **a**-axis parallel to the crystal elongation is oriented in the vertical direction, because the **a**-axis is common through the sector, whereas the **c**-axis-directions are not the same throughout the crystal due to reflection twinning parallel to (001).

Monoclinic stilbite is bounded by the (010), (001), (110) and ($\bar{1}$01) faces, and each face has growth hillocks or striations. A sector is produced by crystal growth on each face, whereas a domain is produced by crystal growth on the vicinal face of the growth hillock or striation; thus a sector consists of many domains. If the crystal symmetry is reduced during growth, a mirror plane in the higher symmetry crystal (stellerite) will change to a reflection twin plane in the lower symmetry crystal (stilbite). There are two possible reflection twin planes in stilbite (crystal class $2/m$), occurring parallel to the mirror planes in stellerite (mmm); in Figure 1, one twin plane is vertical and the other is horizontal. As stilbite is triclinic (Langeman, 1886), a reflection twin plane occurs parallel to (010) as well. Orientation of the vicinal face on the crystal face is controlled by the crystal class mmm of the orthorhombic lattice; corresponding domains are related by the three reflection twin operations. Optical vibration directions of the {110} and {$\bar{1}$01} sectors[1] are shown in Figure 1. The {001} sectors consist of fine twin lamellae parallel to the (001) face, and extinction directions incline only 0.5° to the **a**-axis in the Eyi Ju and Poona specimens.

Thin sections cut in various directions were examined between crossed polars on a universal stage. Extinction angles and $2V$ values are shown in Table 2. Extinction angles from morphological **a**- and **b**-axes were measured using adjacent twin lamellae. Although the optical properties differ among the specimens from the three localities, the surface features and internal textures are similar.

(010) face: the surface of stilbite is composed of many small, thin stilbite crystals grown parallel to the (010) face, whose form is similar to the macro-crystal. The small stil-

[1] Throughout this paper, the Miller indices refer to monoclinic axes, though the interaxial angle β observed by X-ray methods is that of the pseudo-orthorhombic lattice (Passaglia et al., 1978).

0003–004X/85/0708–0814$02.00

Table 1. Chemical analyses, refractive indices (α, β, γ) and crystal sizes of stilbite

	1		2	3
SiO_2	57.97		65.70	56.38
Al_2O_3	15.41		16.13	15.89
TiO_2			nd	nd
Fe_2O_3			nd	nd
MnO			nd	nd
MgO	0.06		nd	nd
CaO	7.97		7.79	7.94
Na_2O	0.24		0.42	1.08
K_2O	0.05		0.03	0.10
$+H_2O$	18.64		12.89	16.23
$-H_2O$			5.89	1.93
Total	100.34		99.89	99.55
α	1.486	001 sector	1.488	1.492
β	1.492		1.496	1.500
γ	1.495		1.498	1.502
α		110 sector	1.488	
β			1.496	
γ			1.497	
crystal size (cm)	1.5x0.5x1		3x0.5x2	1x0.3x0.3

1. Eyi Ju stilbite (Kozu et al., 1937)
   $(Na_{0.22}K_{0.03})(Ca_{4.04}Mg_{0.04})Al_{8.60}Si_{27.45}O_{72}\cdot 29.5H_2O$
2. Poona stilbite
   $(Na_{0.39}K_{0.02})Ca_{3.99}Al_{9.08}Si_{27.09}O_{72}\cdot 29.96H_2O$
3. Bomeki stilbite (Taniguchi and Abe, 1981)
   $(Na_{1.00}K_{0.06})Ca_{4.07}Al_{8.96}Si_{26.98}O_{72}\cdot 28.98H_2O$

bite crystal consists of two large vicinal faces with symmetrical growth steps parallel to m and m(110) faces (Fig. 2). No growth center is observed on the surface, suggesting a two-dimensional growth mechanism.

{010} sector: in thin section, the symmetrical vicinal faces produce two corresponding domains, whose extinction directions incline about 1.5° (Poona specimen) to the **a**-axis, and are in (001) reflection twin relation with each other (Fig. 3). The (110) faces of the small stilbite crystal produce corresponding {110} domains, the optical properties of which are similar to those of the macro-crystal.

(110) face: the crystal has four equivalent (110) faces on the tip, because of (010) and (001) sectorial twinnings. The (110) face is composed of many parallel blocks with fine striations parallel to the **c**-axis.

{110} sector: the section normal to the **a**-axis shows four equivalent {110} sectors, as shown by Langeman (1886). Figure 4 depicts the internal texture of the {110} sector observed in the (010) section. Roughly vertical, thick stripes correlate to the large m and small m(110) faces, and extend through fine growth zoning parallel to the (110) face.

(001) face: the (001) face has fine striations parallel to the **a**-axis. These striations have their origin in the parallel growth on the (010) face, and in the repetition of two vicinal faces inclined symmetrically with respect to the (010) face. The vicinal face is distinctly observed in both Poona and Eyi Ju specimens (Fig. 5), and the face angle is about 9°. The striations are simple and fine in both Poona and Eyi Ju specimens, whereas they are somewhat rough in the Bomeki specimen.

{001} sector: the (010) thin section shows fine twinning parallel to (001). The extinction in the (010) section, which inclines 0.5° to the **a**-axis, is sharp in both Poona and Eyi Ju specimens, whereas it varies within 4° in the Bomeki specimen. In the thin section normal to the **a**-axis, two kinds of domains are observed in lamellae (Fig. 5). The domains are in a twin relation with respect to the (010) plane, and correspond to the vicinal faces on the (001) face. The optical vibration direction *Y* is clearly inclined to the **b**-axis in the three specimens, suggesting triclinic symmetry, although in Langeman's paper (1886, Figures 26, 27 and 28), it is parallel to the **b**-axis. The optical orientation is indicated in Figure 6; the orientation in other sectors is similar to this.

($\bar{1}01$) face: the ($\bar{1}01$) face occurs on the specimens from Bomeki and Eyi Ju, but not on the specimen from Poona. The ($\bar{1}01$) face of Bomeki stilbite is divided into several

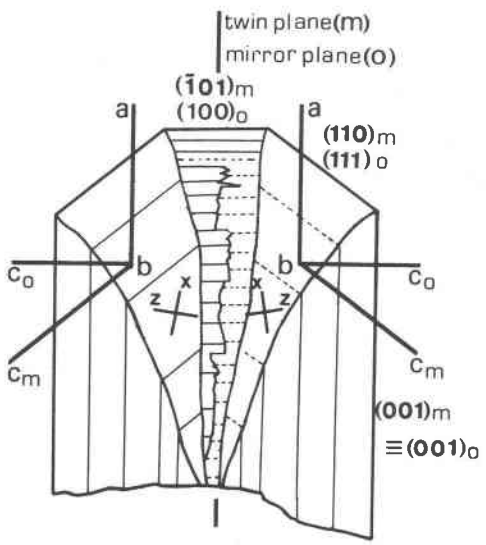

Fig. 1. Schematic sketch of a (010) section of Eyi Ju stilbite. This shows growth sectors and the relation between crystal orientations of monoclinic stilbite (m) and orthorhombic stellerite (o). The $(001)_m$ and $(\bar{1}01)_m$ are normal to the plane of the figure, whereas $(110)_m$ is inclined to the plane of the figure. The {110} and $\{\bar{1}01\}$ sectors, which are indicated by solid and dashed lines, are optically symmetrical with each other. The {001} sectors consist of the fine reflection twins parallel to (001). Optic vibration directions which are symmetrical with respect to the twin plane are represented on the figure.

Table 2. Na + K content, interaxial angle β, extinction angles and $2V_x$ values of stilbite

	$(Na + K)_2O$ (wt. %)	sector	β	extinction a-(010) (±0.5°)	extinction b-($\bar{1}$01) (±0.5°)	$2V_x$ (±1°)
Eyi Ju	0.29	{010}			3.5°	44-45°
		{001}	90.05°	0.5°	3.5-6	43-45
		{110}	90.37	1-2	2-2.5	43
		{$\bar{1}$01}	90.05	0.5	2.5	32-33
Poona A	0.45	{010}		1-4	3	42-44
		{001}	90.05	0.5	8	36-42
		{110}	90.49	3-4	5	35-44
		{$\bar{1}$01}		1	5	23
Poona B	0.87	{010}		1-4	2.5-3	37-42
		{001}	90.05	0.5-1.5	5	36
		{110}	90.49	3.5-5	2.3-3	40-43
		{$\bar{1}$01}				
Bomeki	1.18	{010}			5	32-34
		{001}	90.49	< 4	5	30
		{110}	90.62	6-7	5	35-36
		{$\bar{1}$01}		5	8	22

a-(010) and b-($\bar{1}$01) are extinction angles from a-axis on (010) and from b-axis on ($\bar{1}$01) sections, respectively.

blocks without growth hillocks, whereas the face of Eyi Ju stilbite consists of one or two blocks that have growth hillocks with two curved vicinal faces.

{$\bar{1}$01} sector: although the ($\bar{1}$01) face does not occur on the crystal surface of the Poona specimen, the corresponding sector is found inside crystal B. The {$\bar{1}$01} sector shows fine twinning parallel to the ($\bar{1}$01) face in the (010) section, and the two kinds of twin component frequently cross in a comb-like pattern with each other (Fig. 1). The section normal to the **a**-axis shows a rhombic {$\bar{1}$01} sector (Langeman, 1886, Fig. 27), in which some indistinct domains are observed.

X-ray and chemical analyses

The {001}, {110} and {$\bar{1}$01} sectors were separated from the thick sections normal to the **a**-axis or parallel to (010), and the 204 and 20$\bar{4}$ diffraction peaks (in the pseudo-orthorhombic orientation) were recorded on an X-ray powder diffractometer. Figure 7 shows the 204 and 20$\bar{4}$ diffraction peaks of the {001} and {110} sectors in two different specimens (A and B) from Poona, India. The peak of the {110} sector material is split into two in both specimens A and B, whereas the peaks of {001} sector material are rather sharp as compared with those of {110} sector. From the difference in the diffraction angle ($\Delta = 2\theta_{204} - 2\theta_{20\bar{4}}$), the pseudo-orthorhombic interaxial angles β were calculated from the equation ($90° + 2.466\Delta = \beta \pm 0.05°$)of Passaglia et al. (1978). The β-angle of the {010} sector was not observed, because this {010} sector consists of various kinds of domains. The interaxial angles β are shown in Table 2. The {001} sectors in both Poona and Eyi Ju stilbite crystals are orthorhombic or nearly orthorhombic, whereas the {110} sectors deviate significantly from orthorhombic symmetry. Although both {001} and {110} sectors in Bomeki stilbite are monoclinic, the β angle of the {001} sector is smaller than that of the {110} sector. The peaks are broad, except for those of the {001} sectors of Poona and Eyi Ju stilbite, which are rather sharp; thus the angles shown in Table 2 are average values.

Table 3 shows sodium and potassium contents and the interaxial angle β in the {001} and {110} sectors of the two Poona specimens (A and B). Sodium and potassium contents are the same in both sectors within error, and electron microprobe analyses show that the specimens from the three localities are chemically homogeneous through the sectors. Although Passaglia et al. (1978) suggested that stilbite is chemically heterogeneous, the stilbite crystals studied by us are chemically homogeneous, and structurally heterogeneous. Table 2 shows that the interaxial angle β decreases as the sodium content decreases, and that the angle β of the {001} sector is smaller than that of the {110}

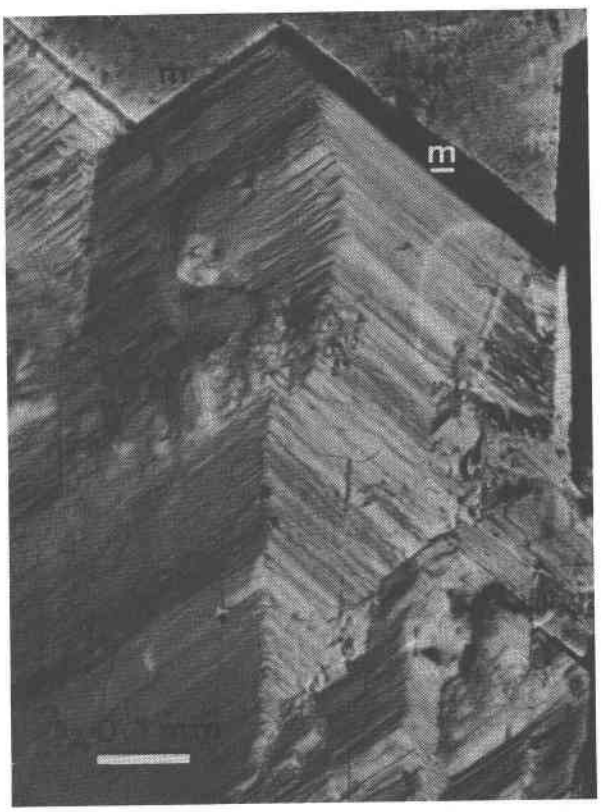

Fig. 2. Reflection interference photomicrograph of small stilbite crystals grown parallel to each other on (010). The surface consists of two vicinal faces with symmetrical steps parallel to m and m(110). The **a**-axis is vertical. Poona stilbite.

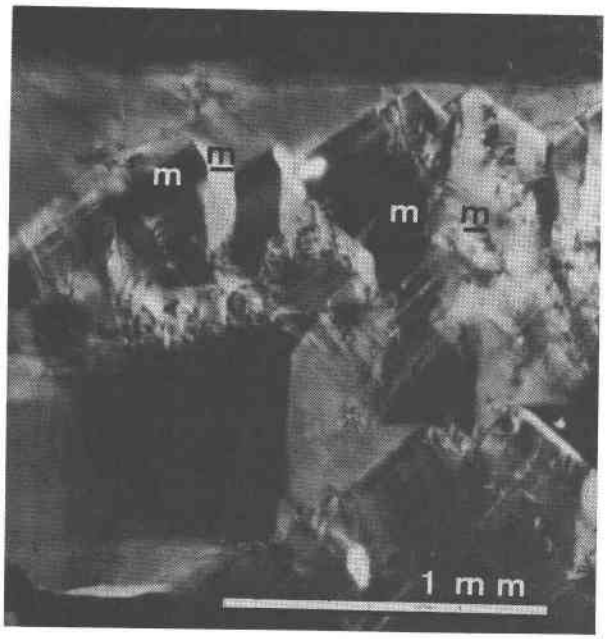

Fig. 3. Cross polarized photomicrograph of a thin section parallel to (010). The domains (m and m) correspond to the vicinal faces of the small crystals on (010), as shown in Fig. 2. The a-axis is vertical. Poona stilbite.

sector. According to the chemical formulae of the three specimens (Table 1), the substitution of sodium (+potassium) for calcium is negligible.

Discussion

In some minerals with growth sectors exhibiting "abnormal optical properties", the optical symmetry of the mineral is the same as the symmetry of the unit cell; if fine-scale polysynthetic twinning is present, the optical symmetry and/or the diffraction symmetry may be enhanced. Although sodium-rich stilbite has been taken as monoclinic in X-ray studies, the true symmetry of the (average) unit cell is triclinic. Correlation between surface growth features and internal textures suggests that the internal textures were produced during growth. The optical properties and internal texture may be interpreted by the atomic order-disorder growth sector mechanism suggested by Akizuki (1981a) for analcime.

Orthorhombic–monoclinic structures

In the crystal structure of stilbite (Fig. 8), calcium ions are near the middle of the channels; they are coordinated by eight water molecules and do not bond to the framework oxygen atoms (Galli, 1971). This suggests that hydrated calcium ions will have a uniform effect on the (Al,Si) sites during growth. Sodium ions coordinate directly with oxygens of the Si(2) and Si(5) tetrahedra (Galli, 1971). This suggests that the sodium ions, which were released from H_2O molecules at the crystal surface, will have a direct influence only on the Si(2) and Si(5) sites during growth, and these will be preferentially occupied by aluminum ions. The Si(5) site shares two oxygens with an adjacent sodium ion, whereas the Si(2) site is linked to one such oxygen. This might suggest the aluminum occupancy of Si(5) to be greater than that of Si(2). Galli and Alberti (1975) suggested that the Si(5) site is preferentially occupied by aluminum.

The principal difference between the orthorhombic and monoclinic structures involves the tetrahedra directly linked to the sodium ions (Fig. 8); these are rotated in a clockwise manner in the monoclinic structure relative to their configuration in the orthorhombic structure. Galli and Alberti (1975) suggest that the cause of the rotation is repulsion between sodium and calcium ions. Consequently it is necessary to consider the effect of sodium on the growth of stilbite. In stilbite, the two sodium ions bond to two O(2) oxygens and some H_2O molecules, and not to O(1) oxygens (Fig. 8). Thus the immediate surroundings of sodium are different on the (110) and (111) faces, that are equivalent in orthorhombic stellerite. The local charge balance will be different on the two faces of stilbite, and a more balanced atomic arrangement may develop during growth. If the clockwise-rotated structure shown in Figure 8 is produced on the m(110) face, the counter-clockwise rotated structure will occur on the symmetrical m(110) face, resulting in monoclinic, twinned {110} sectors (Fig. 3). Because the tetrahedra Si(5a) and Si(5b) have equivalent environments with respect to calcium ions on the (001) face of the orthorhombic structure, the clockwise and counter-

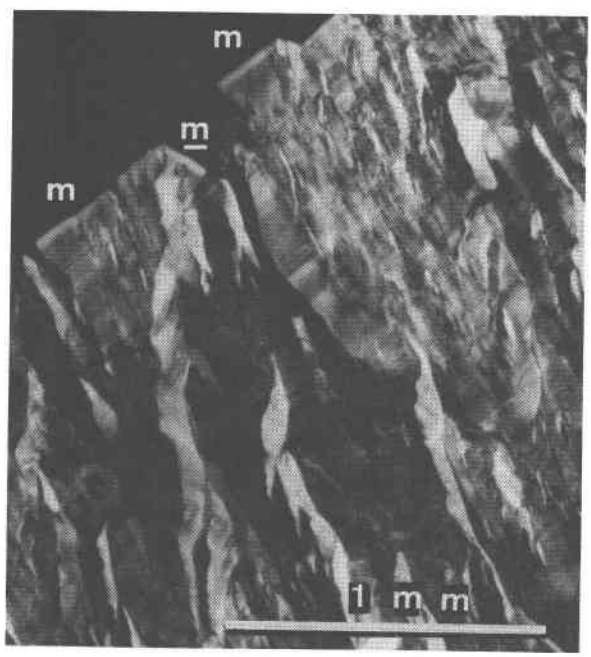

Fig. 4. Cross polarized photomicrograph of m{110} sector in thin section parallel to (010). The m and m{110} faces and corresponding domains are seen. The a-axis is vertical. Poona stilbite.

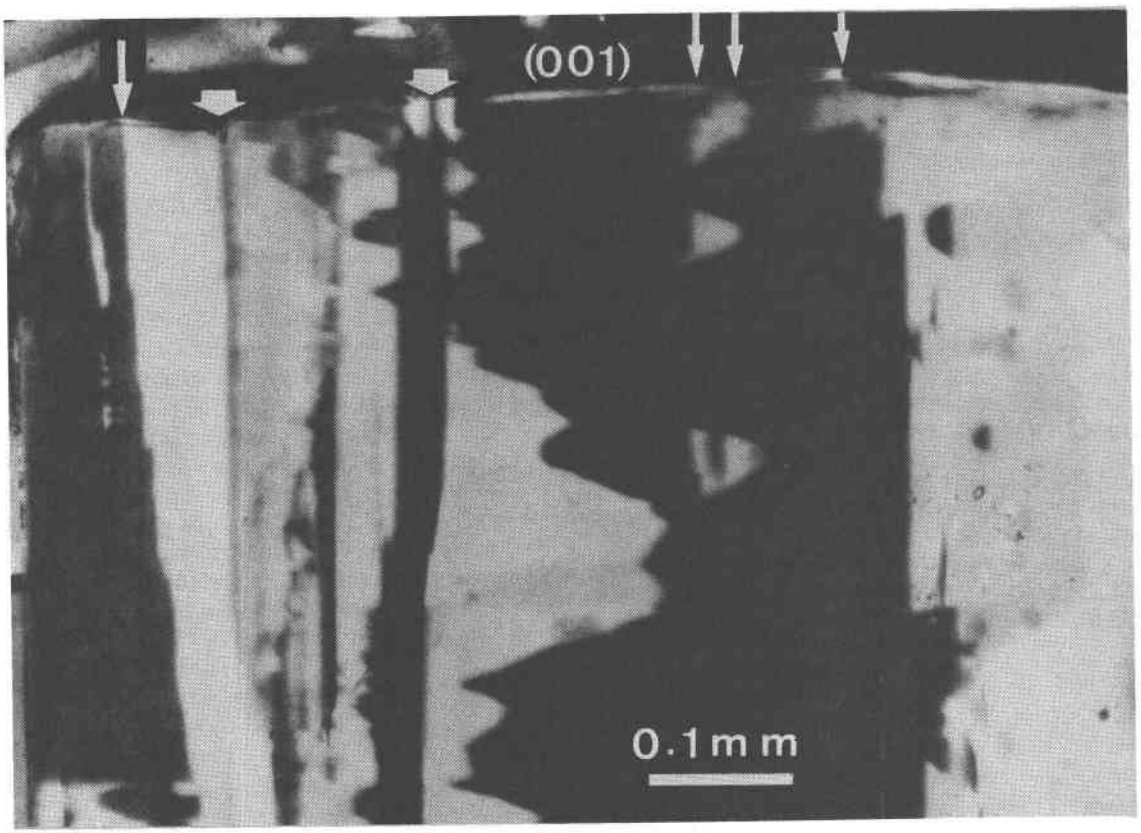

Fig. 5. Cross polarized photomicrograph of a {001} sector in thin section normal to the **a**-axis. The (001) face, which is normal to the paper, kinks at some places shown by thin arrows, and the sector twin plane corresponds to the kink. The thick arrows show contact planes of parallel growth crystals. The **b**-axis is horizontal. Poona stilbite.

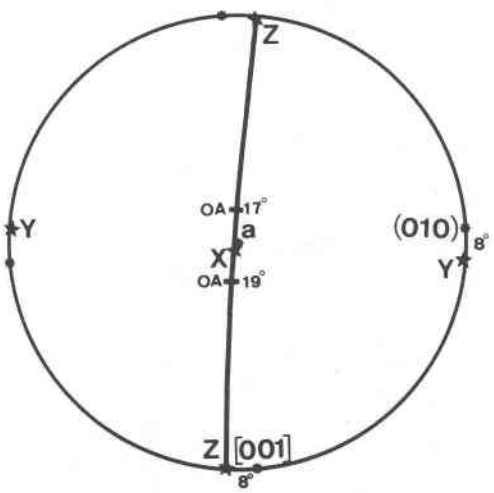

Fig. 6. Stereographic projection of the optical properties of the domain showing black contrast in Fig. 5. The principal vibration directions (X, Y, Z), optic axial plane, optic axes (OA), and **a**-axis (a), are shown. Angles between "OA" and "a" are 17° and 19°, respectively, and $2V_x = 36°$. The X-direction inclines very slightly to the **a**-axis.

clockwise rotations will be produced at the same probability on the (001) face of stilbite, and the {001} sector will consist of a disordered, orthorhombic arrangement. According to Galli and Alberti (1975), repulsive forces between calcium and sodium ions successively rotate adjacent cells with sodium ions in the same direction during growth; this results in a ordered monoclinic structure. However, the Na sites are not always occupied completely by sodium (Galli, 1971). If orthorhombic cells without sodium are produced at growth steps, the following monoclinic cells may rotate either clockwise or counter-clockwise. Thus, in the {001} sector, the rotation direction of the monoclinic cells becomes more disordered as the number of orthorhombic cells (without sodium) increases. The interaxial angle β of the pseudo-orthorhombic lattice closes to 90° in all sectors as the sodium content decreases, and furthermore the angle β of the {001} sector becomes smaller than that of the {110} sectors in the same crystal.

These ideal symmetries are in agreement with those observed by X-ray diffraction and optical microscopy. Stellerite is orthorhombic. The diffraction pattern of a whole stilbite crystal shows a mixture of monoclinic and orthorhombic phases. If the powder pattern is made using a

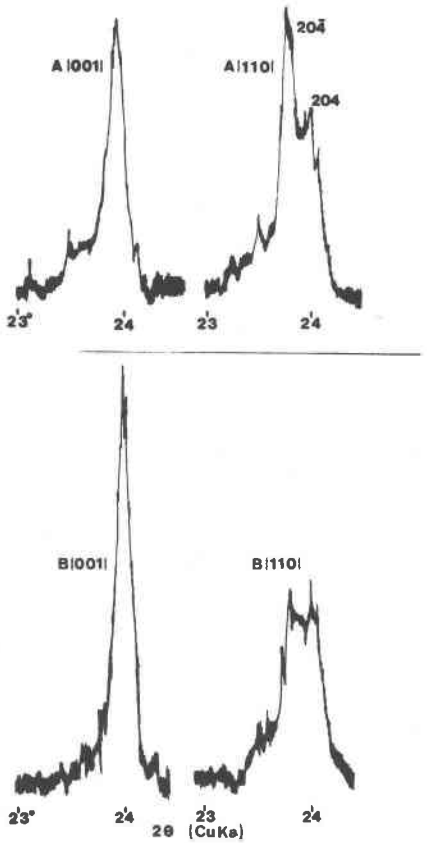

Fig. 7. X-ray diffraction peaks of {001} and {110} sectors in two different specimens from Poona, India.

sector of the large crystal, the pattern will be monoclinic, orthorhombic or mixed. No chemical difference is observed between the {001} and {110} sectors. Passaglia et al. (1978) noted orthorhombic, monoclinic or mixed stilbite from many localities, and suggested that the stilbite is chemically

Table 3. Sodium and potassium contents & internal angle in the {001} and {110} sectors of two different Poona stilbite crystals (A and B).

specimen	sector	Na_2O(wt. %)	K_2O(wt. %)	β
A	{001}	0.44	0.03	90.05°
	{110}	0.40	0.03	90.49°
B	{001}	0.85	0.02	90.05°
	{110}	0.85	0.02	90.49°

The angles $\Delta=2\theta_{204} - 2\theta_{20\bar{4}}$ are measured to be 0.02° and 0.2° in the {001} and {110} sectors, respectively, though the peaks are more or less broad, especially in the {110} sectors. Wet chemical analyses.

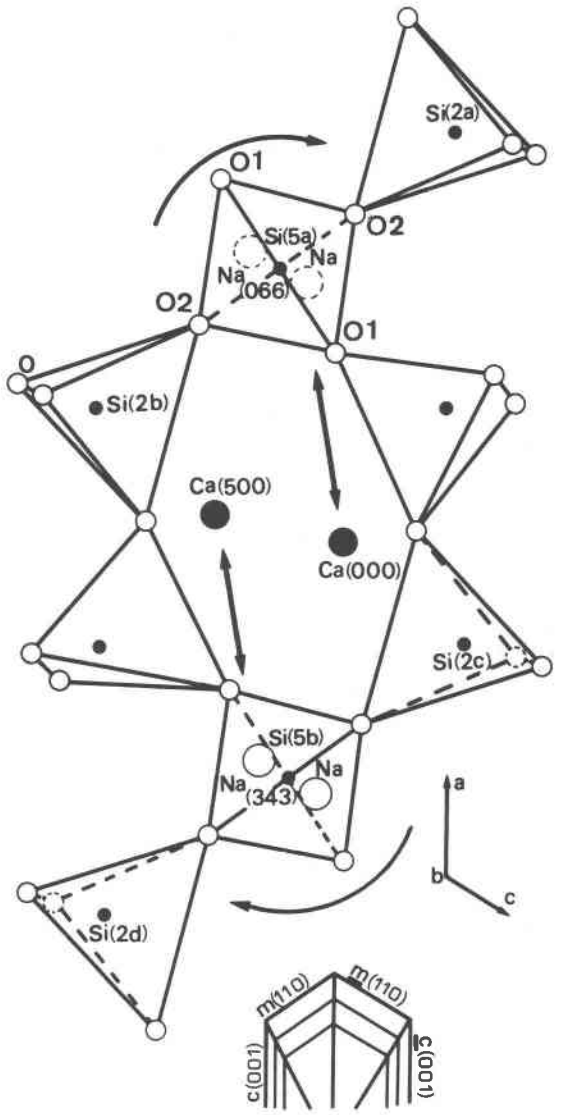

Fig. 8. Part of the structure of stilbite projected along the b-axis. Numbers adjacent to calcium and sodium give the heights of the atoms in thousandths of a cell edge. Rotations of the tetrahedra and sodium atoms are shown by curved arrows. Repulsion between sodium and calcium ions is shown by straight arrows. Also, schematic internal texture is shown below. The m and m(110) are inclined to the plane of the figure, whereas c and c(001) are normal to the plane of figure. Modified from Galli and Alberti (1975).

heterogeneous. We suggest that stilbite is chemically homogeneous but structurally heterogeneous.

Triclinic structure

Small deviations from monoclinic symmetry may be explained by the following mechanism. According to the ideas of Akizuki (1981a), the Si(2) and Si(5) sites each split

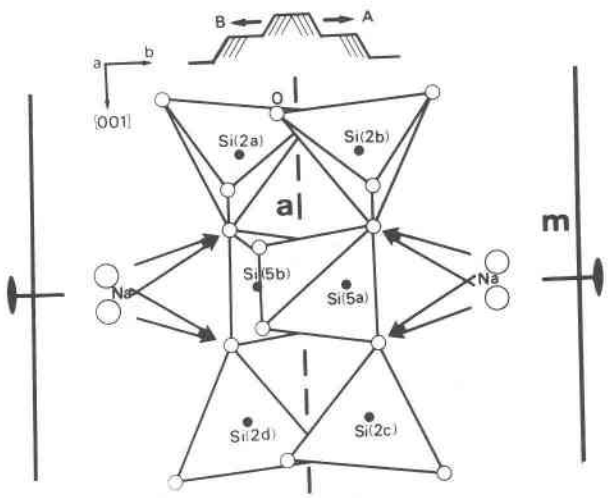

Fig. 9. Part of the structure of stilbite projected along the **a**-axis. The two growth steps (A and B) move on vicinal faces normal to the plane of the figure in the direction shown by small arrows. Oxygen atoms bonded to sodium are shown by four large arrows. Mirror planes are vertical and diad axes are horizontal.

into two sites during growth. Assuming growth to be in the **b**-direction in Figure 8, the Si(5a) tetrahedron forms after the two sodium ions during growth, whereas the Si(5b) forms prior to the sodium ions. This suggests that the Si(5a) site will be preferentially occupied by aluminum due to the local effect of the sodium ions. On the other hand, the Si(5b) site will be occupied by silicon, because the site is produced before the sodium ions. If the crystal grows on m(110), the Si(2a) site will form after the sodium ions and will be occupied by aluminum ions; the Si(2b) site is formed before the sodium ions and will be occupied by silicon. Due to the Al/Si ordering at both the Si(2) and Si(5) sites, the $C2/m$ symmetry is reduced to $C1$ in domains corresponding to the symmetrical vicinal faces on (010) (Fig. 2).

Figure 9 shows a partial view of the stilbite structure normal to the **a**-axis; only the Si(2) and Si(5) tetrahedra are shown. Growth steps normal to the figure are indicated by the letters A and B. If the crystal grows on step A, aluminum ions will preferentially occupy the Si(2a), Si(2d) and Si(5b) sites under the influence of the sodium ions, and silicon ions will occupy the Si(2b), Si(2c) and Si(5a) sites. Also, the aluminum occupancy may be different between the Si(2a) and Si(2d) sites, because the immediate surroundings are different with respect to the Na between the two sites on the surface, and the diad axis disappears from the structure. Thus the {001} sector may triclinic $C1$ and the domains corresponding to the symmetrical vicinal faces A and B are in a twin relation (Fig. 5). Galli (1971) suggested that in stilbite, the Si(5) site splits into two sites, Si(5a) and Si(5b).

The $\{\bar{1}01\}$ sector is similar to the {001} sector, and the structure is orthorhombic or nearly orthorhombic. The $(\bar{1}01)$ face may be not normal to the **a**-axis, and therefore, two symmetrical $f(\bar{1}01)$ and $\underline{f}(\bar{1}01)$ faces are produced in stilbite, resulting in twinned f and $\underline{f}\{\bar{1}01\}$ domains. The growth steps on (010) have many kinks, at which growth directions vary, and fine-scale domains are produced in this sector. Strain will occur along the domain boundaries. As (010), which is a perfect cleavage plane, cuts a minimum number of Si–O–Si and Ca, Na–O bonds (Galli, 1971), growth splitting occurs in the direction normal to the (010) plane during growth, and strain decreases.

Conclusion

The $\{\bar{1}01\}$ and {001} sectors show orthorhombic symmetry due to the disordered rotation of tetrahedra which occur on the side faces of steps formed during growth. The {110} sector is monoclinic due to the ordered rotation of the same tetrahedra. Furthermore, the stilbite structure reduces to triclinic symmetry, because an ordered arrangement of Al/Si occurs during growth. When vicinal faces on the surface are symmetrically inclined to the mirror plane in orthorhombic symmetry, the ordered structures are also symmetrical with respect to the mirror plane, resulting in twinning. On the vicinal face normal to the mirror plane, the corresponding domain becomes statistically disordered, and the mirror plane is maintained during growth. The crystal is chemically homogeneous, and the internal textures occur as a result of this sector growth mechanism.

Acknowledgments

We thank Professor F. C. Hawthorne, University of Manitoba, Canada, for valuable suggestions and English correction of the manuscript. Also, we thank Professor E. Galli, University of Modena, Italy, and Professor R. B. Ferguson, University of Manitoba, Canada, for critical reading of the manuscript.

References

Akizuki, Mizuhiko (1984) Origin of optical variations in grossular–andradite garnet. American Mineralogist, 69, 328–338.

Akizuki, Mizuhiko (1981a) Origin of optical variation in analcime. American Mineralogist, 66, 403–409.

Akizuki, Mizuhiko (1981b) Origin of optical variation in chabazite. Lithos, 14, 17–21.

Akizuki, Mizuhiko (1980) Texture of stilbite from Bomeki, the suburb of Sendai, Japan. Journal of the Japanese Association of Mineralogists, Petrologists, and Economic Geologists, 75, 38–43. (In Japanese).

Akizuki, Mizuhiko and Sunagawa Ichiro (1978) Study of the sector structure in adularia by means of optical microscopy, infra-red absorption, and electron microscopy. Mineralogical Magazine, 42, 453–462.

Akizuki, Mizuhiko, Hampar, M. S. and Zussman, Jack (1979) An explanation of anomalous optical properties of topaz. Mineralogical Magazine, 43, 237–241.

Breck, D. W. (1974) Zeolite Molecular Sieves. John Wiley & Sons, Inc.

Černý, P. (1964) Ionic substitutions in natural stilbite. Neues Jahrbuch für Mineralogie, 1965, 198–208.

Galli, Ermanno (1971) Refinement of the crystal structure of stilbite. Acta Crystallographica, B27, 833–841.

Galli, Ermanno and Passaglia, Elio (1973) Stellerite from Villanova Monteleone, Sardinia, Lithos, 6, 83–90.

Galli, Ermanno and Alberti, Alberto (1975) The crystal structure of stellerite. Bulletin de la Société francaise de Minéralogie et du Cristallographie, 98, 11–18.

Kerr, P. F. (1977) Optical Mineralogy, 4th ed. McGraw-Hill Book Company, New York.

Kozu, Shukusuke, Seto, Kunikatsu and Kawano Yoshinori (1937) New occurrence of stellerite from Eyi Ju Mine. Journal of the Japanese Association of Mineralogists, Petrologists, and Economic Geologists, 18, 51–58. (In Japanese)

Langeman, Ludwig (1886) Beiträge zur Kenntniss der Mineralien: Harmotom, Phillipsit und Desmin. Neues Jahrbuch für Mineralogie, Geologie und Palaeontologie, 2, 83–141.

Passaglia, Elio, Galli, Ermanno, Leoni, Leonardo and Rossi, Giuseppe (1978) The crystal chemistry of stilbites and stellerites. Bulletin de Minéralogie, 101, 368–375.

Slaughter, Maynard (1970) Crystal structure of stilbite. American Mineralogist, 55, 387–397.

Taniguchi, Masahiro and Abe Tomohiko (1981) Stilbite from Bomeki, Miyagi Prefecture, Japan. Journal of the Japanese Association of Mineralogists, Petrologists and Economic Geologists, 76, 324–330.

Manuscript received, March 27, 1984;
accepted for publication, February 5, 1985.